

Hydrogenation of Carbon Nanotubes: Roles of Symmetry and Strain

Kun Xue¹ and Zhiping Xu^{2,*}

¹ State Key Laboratory of Explosion Science and Technology, Beijing Institute of Technology, Beijing 100081, China

² Department of Civil and Environmental Engineering, Massachusetts Institute of Technology, Cambridge 02139, MA, USA

* Email: xuzp@mit.edu

Abstract: Carbon nanotube is excellent material for hydrogen storage and molecular sensory applications thanks to its quasi-one dimensional geometry and unique structure-property relationship. In this paper, hydrogenation of carbon nanotubes is discussed in the extent of binding geometry and mechanochemical coupling under structural deformation. Our first-principles calculations show that the atomic structures, mechanical and electronic properties of carbon nanotubes can be significantly modified by hydrogenation. Moreover, the hydrogenation process is controlled by strain loading. Under an axial compressive or tensile strain of 10 %, the binding energies of hydrogen on carbon nanotubes can be changed up to -0.24 and 0.74 eV respectively. Analysis on electronic structure, mechanical properties and charge density reveals the underline mechanisms. The results reported here offer a way not only to tune the binding strength of hydrogen on carbon nanotubes in a controllable and reversible manner, but also to engineer the properties of carbon nanotubes through a synergistic control on hydrogen binding and mechanical loading.

Keywords: carbon nanotubes, hydrogen storage, strain engineering, electronic properties, mechanical properties

1 INTRODUCTION

Carbon nanostructures, such as carbon nanotube and graphene, are mono-atomically layered material, possessing fascinating electronic and mechanical properties [1]. Besides of its intrinsic properties, there have been arising interests and efforts in the physical chemistry of carbon nanostructures recently, especially in the extent of molecular doping and sensing by hydrogen, oxygen, NO₂, NH₃ et al. [2-5]. The notion of doping, covalently or non-covalently, has been renovated in a controllable and reversible manner thanks to the co-existence chemical inertness of sp^2 carbon network and relative activity of their π electrons. Molecular sensors have been proposed according to their significant response in electronic properties under various chemical stimulations. This remarkable structure-property sensitivity also inspires engineering on the carbon nanostructures through chemical functionalization. Hydrogenation [6, 7] and epoxidation [8, 9] are two of the most noticeable approaches in this direction. In special, hydrogenation has great potential applications in hydrogen storage industry. Fully hydrogenation of sp^2 bonded carbon nanostructures provides high hydrogen storage weight ratio up to 7.7 wt %, which is able to meet DOE's 2010 goal (6 wt %). The modification on the sp^2 structure in carbon nanotubes is able to introduce dramatic changes in their structural and electronic properties. For example, recent experiment has shown a metal-semiconductor transition [7] in graphene sheets upon hydrogenation. More interestingly, the metallic characteristic and other properties of intrinsic graphene sheet can be recovered after structural annealing later on [7]. The controllable and reversible hydrogenation of carbon nanostructures is very promising for the hydrogen storage industry, because novel and flexible controls on the hydrogen binding and releasing are extremely critical in the applications. Future development following this concept relies upon our understanding on the mechanism of reversible hydrogenation process and the roles of external control such as strain loading, thermal treatment or electromagnetic fields. In this paper, we focus on the mechanism of carbon nanotube hydrogenation under mechanical loads, from a synesthetic viewpoint in both structural and electronic aspects.

2 METHODS

The structural and electronic properties of both pristine and hydrogenated armchair carbon nanotubes are investigated through first-principles calculations here. Hydrogen atoms are initially assigned on the carbon atoms on nanotubes along radial direction. A guess bond length l_{C-H} of 1 Å is used. The atomic structure is optimized then to provide starting point for following calculations on material properties. In our work, plane-wave basis sets based density functional theory (DFT) is employed using generalized gradient approximation (GGA) with PBE functional for exchange-correlation terms [10]. Ultrasoft pseudopotentials are implemented for the ion-valence electron interactions. We used the PWSCF code [11] for the calculation. For all the results presented in this paper, energy cut-offs of 30 Rydberg and 240 Rydberg are used for plane-wave basis sets and charge density grids respectively. The settings are verified to achieve a total energy convergence less than 10^{-5} Ry/atom. The structural optimization is performed with maximum force on atom criteria set to be 0.001 Ry/Å. For variable-cell relaxation along the nanotube axis, the criteria for stress is set to be 0.01 GPa and. Sixteen Monkhorst-Pack k-points are used along the

carbon nanotube axis for Brillouin zone integration, which is qualified for the energy convergence criteria of 3 meV.

3 RESULTS AND DISCUSSION

3.1 Structure of Hydrogenated Carbon Nanotubes

The hydrogenation of carbon nanostructures has been widely studied by both experimental methods and quantum mechanical calculations [2, 3, 6, 7, 9, 12]. It is found that hydrogen atoms form covalent bonds with carbon atoms in graphene sheet. The binding energy is on the order of few eV per C-H atom pair. In carbon nanotubes, there are two nonequivalent carbon atom positions A and B in hexagonal graphene lattice (Figure 1). When the hydrogen atoms are accessible to both sides of the graphene sheet, they will bind to A and B on opposite sides to lower total energy. Moreover, grouping into clusters can further reduce the energy of lattice distortion after hydrogenation. While when only one of surfaces is accessible, hydrogen atoms binding A and B sites will be on the same side. So according to the accessible surfaces to gas-phase hydrogen atoms or H₂ molecules, final structures formed will have different symmetries.

To the maximum extent possible, carbon nanostructures can be fully hydrogenated with the ratio between numbers of carbon and hydrogen atoms C:H = 1:1. In this work, we take this limit. Two structures that maximize the hydrogen storage capacity are investigated. According to the binding pattern symmetry of hydrogen atoms on sublattices A and B, we refer to the structure with hydrogen atoms binding on the same side of graphene sheet as *symmetric* structure (Figure 1(a)) and on the opposite sides as *antisymmetric* structure (Figure 1(b)). For the symmetric structure, only outer surface is exposed to the hydrogen-rich environment, while in the antisymmetric structure the inner surface becomes also available, this is the case when the ends of carbon nanotubes are opened [13]. In our calculation, one unit cell of armchair carbon nanotubes (n, n) along axis is used to represent the whole tube. The unit cell contains $4n$ carbon and $4n$ hydrogen atoms, and has an axial lattice constant a . A vacuum layer of 20 Å in the transverse direction is used to avoid interaction between neighboring nanotubes.

The geometries of both symmetrically and antisymmetrically hydrogenated carbon nanotubes are optimized following a variable cell approach to release axial stress built in. The optimized lattice constant for pristine (5,5) carbon nanotube is 2.45 Å, which is expanded to 2.62 and 2.58 Å in the symmetric and antisymmetric structures after hydrogenation. Antisymmetric structure with relaxed lattice constant is found to be energetically 0.56 eV (per carbon-hydrogen pair) more favorable than the symmetric one. Figure 2 shows the electron densities of symmetric and antisymmetric structures in comparison with the pristine (5,5) carbon nanotube. The difference shows distinct characteristics of sp^2 graphene and sp^3 diamond characteristics respectively [6]. In the symmetric phase (Figure 1(a)), binding of hydrogen atoms expands the lattice constant of underneath hexagonal graphene lattice but preserves the cylindrical geometry according to the symmetry between binding sites A and B. The carbon-carbon bond length in the circumstantial directions d_{C-C} increases from 1.43 Å to 1.59 Å in the presence of carbon-hydrogen binding. Length d'_{C-C} of other carbon-carbon bonds increases from 1.42 Å to 1.57 Å. These bonds are stretched by 10.34 % and 11.86 % respectively after hydrogenation. The spatial distribution of electron density

in Figure 2(b) shows that p_z orbital of the carbon atom is bonding with hydrogen atoms. As a result, the zero-gap band structure in pristine (5,5) carbon nanotube from π and π^* bands are opened to be $E_g = 2.32$ eV, which is close to the one calculated in symmetrically hydrogenated graphene [6].

In the antisymmetric phase, symmetry breaking between the two representative carbon (hydrogen) atoms A and B in the unit cell destructs the sp^2 hybridization and introduces sp^3 features. This transition does not occur in the symmetric phase because of the local tetrahedral structure is not allowed by symmetry. The carbon-carbon bond lengths here in circumstantial (d_{C-C}) and axial (d'_{C-C}) direction are also elongated to 1.56 and 1.55 Å respectively, close to 1.54 Å in diamond structure. The bond angle between carbon and hydrogen atoms also resembles the tetrahedral symmetry in diamond. The antisymmetric phase has a band gap of 3.61 eV (Figure 2(c)) that is lower than that in diamond (4.2 eV from our DFT calculation). The electronic structure modification is similar to the situation in hydrogenation of graphene [6].

Changing of binding nature in carbon nanotubes also has noticeable impacts on their mechanical properties. Axial Young's moduli Y are calculated for these structures by applying tensile and compressive strain up to 0.01. Pristine and hydrogenated carbon nanotubes are considered as elastic shells with the diameter of 3.43 Å (from pristine nanotube) for comparison. The intershell distance of multiwalled carbon nanotube 3.2 Å is used as the thickness of single-walled carbon nanotube in virial stress calculation. The obtained result for pristine (5,5) carbon nanotubes is 1.092 TPa that is very close to in-plane modulus of graphene sheet [6]. After hydrogenation, the elongation of bond length results in much lower stiffness, i.e. $Y = 666.304$ for symmetric structure and 632.489 GPa for antisymmetric structure with softer sp^3 bonds. These values are even lower if we take into account for the diameter and thickness changes after hydrogenation.

3.2 Binding Energy

To characterize the binding strength between the hydrogen atoms and carbon nanotubes, we define the formation energy of hydrogenated carbon nanotubes as $E_f = [E_{CNT-H} - (E_{CNT} + E_H)]/N_{C-H}$, where E_{CNT-H} and E_{CNT} are the energy of hydrogenated and pristine carbon nanotubes respectively and N_{C-H} is the number of carbon-hydrogen pairs. Negative formation energy means the chemisorption is feasible. E_{CNT} is calculated after geometrical optimization of the bare carbon nanotube structure. The reference energy values for isolated atomic hydrogen atom ($E_H = -13.01$ eV) and hydrogen atom in H_2 molecule ($E_H = -15.85$ eV) that are calculated here are both considered in following discussion. In absence of strain in the (5,5) carbon nanotube, i.e. at $a = 2.45$ Å, symmetrically and antisymmetrically hydrogenated phases have binding strengths E_f of -2.78 and -3.37 eV per C-H atom pair.

The elongation of carbon-carbon bond length and expansion of lattice constant upon hydrogenation suggest that there is significant stress build-up during the hydrogenation when the deformation along axial direction is constrained. We calculate axial stress in armchair carbon nanotubes of various diameter (from (3,3) to (10,10)) with the same constrained lattice constant $a = 2.45$ Å. The results plotted in Figure 3 show that there is considerably high compressive stress built up from 20 to 60 GPa, following the same approach as in the previous Young's modulus calculation. The amplitude of stress depends on the curvature of carbon nanotube and also converges to a constant

value as the diameter increases, which reflects the situation of hydrogenation on graphene sheet [6]. In the symmetric phase of graphane, hydrogen atoms bind on one side of the underline graphene sheet and tend to bend it [6]. Thus hydrogenation of carbon nanotubes prefers those with smaller diameters. As a result, there is more axial stress build-up as the diameter increases. However, in the antisymmetric phase, as hydrogen atoms are binding on both sides, there is no curvature preference. The size-dependence shown in Figure 3 comes from repulsion between the dense carbon-hydrogen bonds inside carbon nanotubes. For the smallest (3,3) nanotube, although there is still enough space for inward carbon-hydrogen bonds, the highly packed structure results in a large axial stress even higher than the symmetric structure. These remarkable mechanical responses upon chemical stimulation imply that possible control of the hydrogenation process and the properties through applying mechanical deformation will be feasible. We thus propose here to engineer through applying *a priori* axial strain on the pristine carbon nanotube.

Starting from the pristine or hydrogenated structures with the same lattice constant, we scale a and optimize corresponding atomic coordinates without changing the size of unit cell. Total energy and axial stress built up in carbon nanotube are calculated using the optimized coordinates. The mechanical stability of carbon nanotubes holding tensile stress is limited by covalent bond breaking down at critical tensile strain, which is 0.16 for single-walled carbon nanotubes as measured experimentally [1] and around 0.20 from theoretical calculations. On the other hand, under compression the strain energy stored in carbon nanotube can be released when it buckles. The critical axial load for Euler buckling is estimated to be $P_c = 4\pi^2 YI/L^2$ when both ends are fixed [14], where I is area inertia of moment and L is the length of carbon nanotube. The maximum compressive strain without buckling can be tuned by the length. For a single-walled (5,5) carbon nanotube with $L = 10$ nm, the critical compressive strain is estimated to be 0.03. Based on these considerations, we limit the scaling of a to be within the range between 2 and 3 Å. As shown in Figure 4, the energy of both pristine carbon nanotube (with additional energy terms for hydrogen atoms) and hydrogenated carbon nanotube changes significantly as strain is applied. Because of the lowering of stiffness in hydrogenated carbon nanotube and changing in lattice constant upon hydrogenation, the energy dependences on strain in various structures are differently, which means the binding energy of hydrogen changes by strain loading. For the symmetrical structures, the binding strength is changed by -0.24 in 10 % compressive and 0.74 eV at 10 % tensile strain. The energy of hydrogenated carbon nanotube is lower than pristine carbon nanotube and hydrogen in atomic phased, giving a favorable negative binding strength. However if the energy of hydrogen atom in H₂ molecule phase is used in calculating E_f , the binding strength is positive when a is below 2.9 Å. Under this environment, a viable way to activate the hydrogen chemisorptions must be found. One possible approach is to utilize the spillover process [15], where H₂ molecules firstly dissociate at the surface of catalyst nanoparticles deposited on the nanotube surface. The hydrogen radicals then spill over from the catalyst to carbon nanotubes and finalize the hydrogenation process. Our results show that when isolated hydrogen atoms is available, the binding strength at 10 % compressive or tensile strain can be changed by -8.5 % and 26.7%. These changes are considerably high. Further tuning on the Gibbs free energy change upon hydrogenation can be achieved by controlling environmental temperature and pressure.

In the antisymmetric structure, the optimized lattice constant $a_{\text{asym}} = 2.58 \text{ \AA}$. A remarkable dependence of the formation energy on the strain is also found (Figure 4). Negative binding strength is observed for a ranging from 2 to 3 \AA if energy of atomic hydrogen is used as the reference. Comparing with previous results for symmetric structures, these results shows that antisymmetric structure is more favorable for hydrogen storage. If molecular hydrogen energy is used, binding is favorable when the lattice constant is larger than 2.3 \AA . Axial strain loading of 10 % compression or tension then gives a change of 0.16 eV per C-H pair. This modification corresponds to 4.7 % of the binding strength at $a = 2.45 \text{ \AA}$ when comparing with pristine carbon nanotube and atomic hydrogen, or 112 % when energy of molecular hydrogen is used for reference. This ultra-sensitivity of hydrogenation on strain loading is very promising to achieve a controllable and reversible process, through a combinational control of strain, temperature and pressure. To this end, procedures to fabricate carbon nanotube membranes with opened ends becomes the key [13].

4 CONCLUSION

In conclusion, we investigate the mechanochemical effects on hydrogenation of carbon nanotubes. The focus is placed on the role of binding symmetry and strain effects on the binding strength. We find that mechanical deformation has remarkable effects on their binding strength: an axial compressive or tensile strain of 10 % can induce up to -0.24 and 0.74 eV change in the binding strength on (5,5) carbon nanotube. The understanding of the underline structural-property relationship thus obtained is of critical importance for hydrogen storage applications, by introducing tunable or even reversible controls. Moreover, the binding of hydrogen on carbon nanotubes opens significant band gaps, reduces stiffness of carbon nanotubes remarkably. Thus the observations here also suggest novel approaches for engineering carbon nanomaterials [16] and rational design of functionalized devices such as chemical sensors.

REFERENCES

- [1] M. S. Dresselhaus, G. Dresselhaus, and P. Avouris, *Carbon nanotubes: synthesis, structure, properties and applications* (Springer, New York, 2000).
- [2] C. Liu *et al.*, *Science* **286**, 1127 (1999).
- [3] A. Nikitin *et al.*, *Nano Letters* **8**, 162 (2007).
- [4] P. G. Collins *et al.*, *Science* **287**, 1801 (2000).
- [5] J. Kong *et al.*, *Science* **287**, 622 (2000).
- [6] K. Xue, and Z. Xu, *Applied Physics Letters* **96** (in press) (2009).
- [7] D. C. Elias *et al.*, *Science* **323**, 610 (2009).
- [8] D. W. Boukhvalov, and M. I. Katsnelson, *Journal of the American Chemical Society* **130**, 10697 (2008).
- [9] Z. Xu, and K. Xue, *Nanotechnology* **21**, 045704 (2009).
- [10] J. P. Perdew, K. Burke, and M. Ernzerhof, *Physical Review Letters* **77**, 3865 (1996).
- [11] PWSCF (distributed in Quantum-Espresso package) is a community project for high-quality quantum-simulation software, based on density-functional theory, and coordinated by Paolo Giannozzi. See <http://www.quantum-espresso.org>

and <http://www.pwscf.org>.

[12] T. Yildirim, O. Gulseren, and S. Ciraci, *Physical Review B* **64**, 075404 (2001).

[13] Y. Zhao *et al.*, *Advanced Materials* **20**, 1772 (2008).

[14] S. P. Timoshenko, and J. M. Gere, *Theory of elastic stability* (McGraw-Hill, New York, 1961).

[15] A. D. Lueking, and R. T. Yang, *Appl. Catal. A* **265**, 259 (2004).

[16] A. K. Singh, and B. I. Yakobson, *Nano Letters* **9**, 1540 (2009).

FIGURES AND CAPTIONS

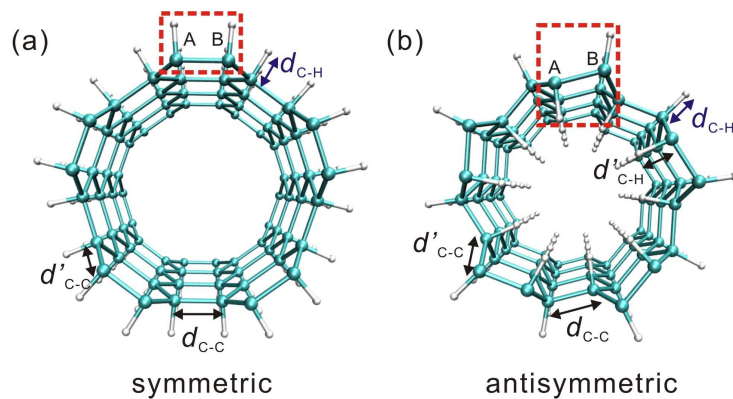


Figure 1. (a) and (b) Optimized structures of symmetrically and antisymmetrically hydrogenated (5,5) carbon nanotube. Four repetitions of the unit cells are shown axially. The two carbon-hydrogen atom pairs A and B in inequivalent sublattices are highlighted in red dash box. The structure of symmetric hydrogenated carbon nanotube significantly expands (with a radius $R = 3.94 \text{ \AA}$ for the carbon atom ring) in comparison with pristine structures ($R = 3.43 \text{ \AA}$). The carbon-hydrogen bond ($d_{\text{C-H}} = 1.10 \text{ \AA}$) that is perpendicular to the underneath sp^2 carbon-carbon bond suggests π characteristics. The lengths of circumstantial ($d_{\text{C-C}}$) and parallel ($d'_{\text{C-C}}$) carbon-carbon bonds are 1.595 and 1.562 \AA . The antisymmetric structure is less expanded and corrugated into double carbon ring structure ($R = 3.81$ and 3.37 \AA respectively). The carbon-hydrogen pairs pointing outward and inward have similar bond length 1.104 and 1.106 \AA . The lengths of carbon-carbon bonds ($d_{\text{C-C}}$ and $d'_{\text{C-C}}$) are 1.564 and 1.560 \AA .

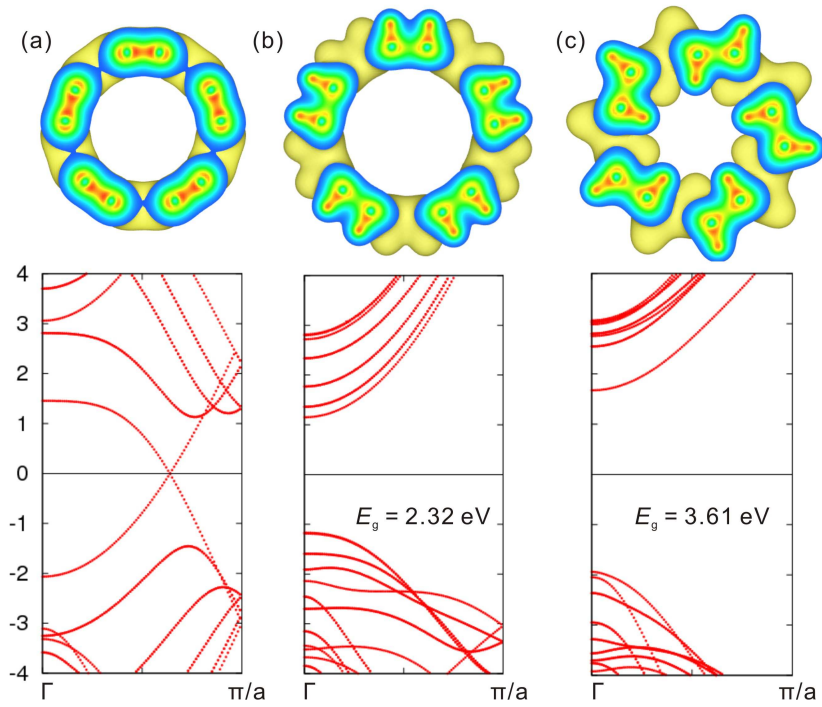


Figure 2. Electron densities and band structures in (a) pristine, (b) symmetrically, and (c) antisymmetrically hydrogenated (5,5) carbon nanotubes. A contour in the plane containing the carbon ring is shown in addition to spatial isosurface plot. Band gap E_g is opened in hydrogenated carbon nanotubes in comparison to the zero-gap band structure in pristine nanotube.

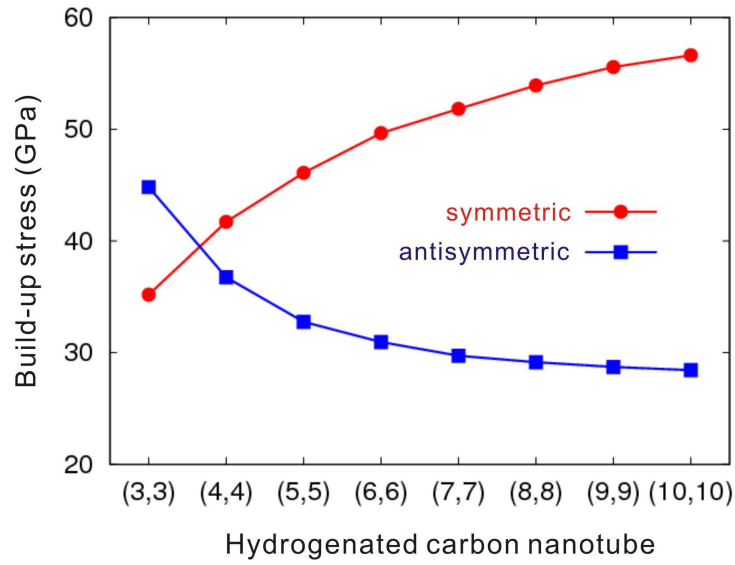


Figure 3. Axial stress built up in hydrogenated carbon nanotubes with various diameters. In symmetric structures (red line + filled circle), the binding of hydrogen tends to bend sp^2 structures and prefers smaller carbon nanotube with larger curvature. While in antisymmetric structures (blue line + filled box), the compact space inside carbon nanotube drives a high axial stress in smaller carbon nanotubes.

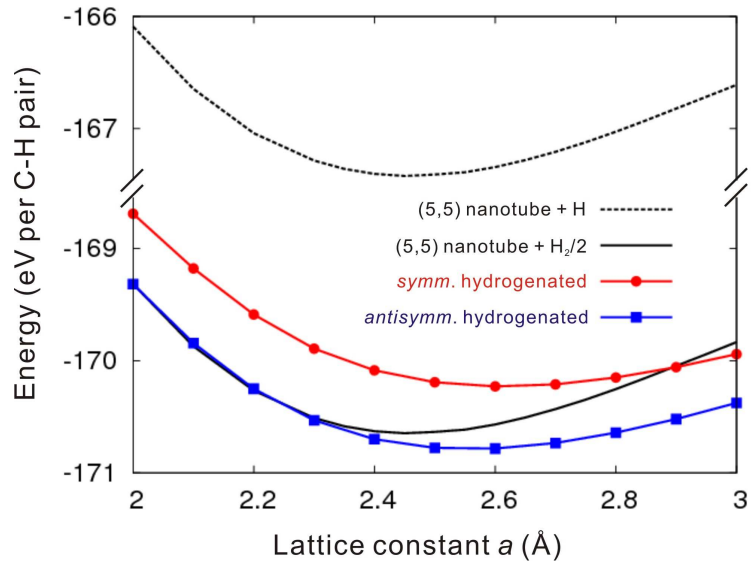


Figure 4. Energy for each carbon-hydrogen pair in different structures investigated for comparison and calculation of cohesive strength. Dash and solid lines show energy of carbon atom in pristine (5,5) nanotube plus hydrogen atom in isolated and H₂ molecule phase. The energy axis ticks are adjusted for a compact illustration. Because of the stiffness softening and lattice constants change upon hydrogenation, the relative changes of energy with respect to axial deformation are different between symmetric (red line + filled circle) and antisymmetric (blue line + filled box) structures.